2012-2-8

Coherent Emission from a Disordered Organic Semiconductor

S. Aberra Guebrou, *et al.*

Coherent Emission from a Disordered Organic Semiconductor Induced by Strong Coupling with Surface Plasmons

S. Aberra Guebrou,[1] C. Symonds,[1] E. Homeyer,[1] J. C. Plenet,[1] Yu. N. Gartstein,[2] V. M. Agranovich,[3,4] and J. Bellessa[1,*]

[1]*LPMCN, Université de Lyon, Université Lyon 1 and CNRS, UMR 5586, F-69622 Villeurbanne, France*

[2]*Physics Department, University of Texas at Dallas, Richardson, Texas 75080, USA*

[3]*Chemistry Department, University of Texas at Dallas, Richardson, Texas 75080, USA*

[4]*Institute of Spectroscopy, Russian Academy of Sciences, Troitsk, Moscow Region, 142190, Russia*

(Received 7 June 2010; revised manuscript received 29 September 2011; published 8 February 2012)

In this Letter, we show that the strong coupling between a disordered set of molecular emitters and surface plasmons leads to the formation of spatially coherent hybrid states extended on macroscopic distances. Young-type interferometric experiments performed on a system of *J*-aggregated dyes spread on a silver layer evidence the coherent emission from different molecular emitters separated by several microns. The coherence is absent in systems in the weak-coupling regime demonstrating the key role of the hybridization of the molecules with the plasmon.

DOI: 10.1103/PhysRevLett.108.066401 PACS numbers: 71.36.+c, 42.25.Kb, 73.20.Mf, 78.55.Kz

Localized and delocalized surface plasmon (SP) modes feature stronger confined electric fields and can therefore efficiently interact with molecules or semiconductors close to metallic interfaces [1,2]. This effect has been widely used to modify optical properties of different types of emitters [3] resulting in radiative rate enhancement and strong coupling. Another important but less studied aspect is the interaction between different emitters induced by SPs. Efficient energy transfer between donor and acceptor molecules on opposite sides of metal films has been demonstrated [4], the transfer being mediated by symmetric and antisymmetric SP modes on a metallic film. A cooperative emission, similar to Dicke superradiance, of an ensemble of dipoles in the vicinity of a metallic nanosphere has also been theoretically identified [5].

The strong-coupling regime offers an interesting perspective for molecular coupling [6] and collective emission. This regime has been reported in various disordered materials such as aggregated dyes coupled to a cavity photon [7] and organic materials [8–11] and semiconductor quantum dots [12] interacting with SPs. Despite the difference of electronic properties of the emitting species in these systems, they all can be seen as a set of localized (no well-defined wave vector) emitters coupled to a propagating extended mode. The strong interaction between a disordered medium and an electromagnetic wave in microcavities has been shown theoretically [13] to result in hybrid eigenstates that are quantum superpositions of a photon and excitations on a large number of molecular sites. Experimentally, the strong coupling is usually identified via observations of an anticrossing in the dispersion relation. The dependence of the Rabi splitting on the concentration of emitters is a good indication of collective effects; however, the coherence of spatially remote emitters induced by hybridization with a plasmon (or cavity) mode has never been directly evidenced. In fact, as was theoretically illustrated [14,15], disorder may result in relatively small modifications of the energetic spectrum of hybrid states, polaritons, while drastically affecting the extent of the polariton wave function.

In this Letter, we specifically address the issue of spatial coherence and find experimental evidence that the strong interaction between a set of molecular emitters and a SP can lead to the formation of a macroscopic extended coherent state akin to that in a macroscopic polymer chain [16]. In the first part of the Letter, we investigate the diffusion and the spatial coherence of the emission of *J*-aggregated dyes on silver with Young-type interferometric experiments, evidencing an in-phase emission of localized emitters separated by several microns. In the second part, the extension of the polaritonic sates is studied and compared to calculations. The extension of such coherent states over a large number of molecules can conceivably be of significance for long-range energy transfer as well as for new optical alloys where the properties of different kinds of emitters spatially separated on a metal film would be mixed via the plasmon.

Our experiments were performed by using a leakage radiation (LR) microscopy setup [17], presented in Fig. 1(a). The samples are excited with a laser light at 532 nm focused on the top side of the sample. The LR of the emission through the silver layer is collected with an immersion oil microscope objective (N.A. = 1.49) placed in contact with the bottom side of the sample and imaged either on a CCD camera or on a CCD detector associated with a spectrometer. A notch filter at 532 nm suppresses the laser radiation in the images. The LR microscopy technique allows a Fourier space imaging providing the angular dispersion of the radiated emission [18] as well as a direct imaging of the emission. In this latter case, a beam block can be inserted in the Fourier plane of the collection optics in order to filter the radiated wave vectors, enabling a

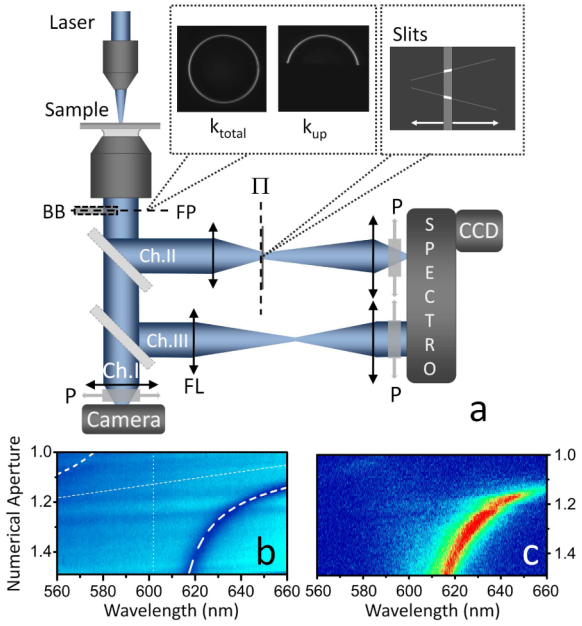

FIG. 1 (color online). (a) Experimental setup. A direct imaging is performed on channel I. Channel II is devoted to coherence measurements by inserting slits in an intermediate image plane Π of the sample surface. Channel III is used for dispersion measurements, by imaging the Fourier plane of the microscope objective on the entrance slit of the spectrometer. A beam block (BB) can be inserted in the Fourier plane (FP) to select a given wave vector direction for all the channels. (b) Reflectometry and (c) luminescence spectra of a TDBC dye layer on a silver film (sample C), displayed as a function of the wavelength and of the numerical aperture (channel III). The dotted lines correspond to the bare plasmon and exciton wavelengths, and the dashed line to the calculated polaritonic dispersion.

selective imaging of the SPs propagating in a given direction. During this study, the experiments were conducted by collecting either all the wave vector components of LR (k_{total} configuration) or solely the wave vector components corresponding to a propagation in the upper half-space as shown in the inset in Fig. 1(a) (k_{up} configuration).

Coherence of the electric field pattern on metal surfaces is associated with highly delocalized surface modes. This coherence is related to the spatial propagation of the SP but not to the coupling as such between different emitters. This phenomenon has been observed in the infrared range [19] for thermal emitters but can also be present in the optical range [20]. In order to clearly evidence the effect of the SP-exciton hybridization, samples in the weak- and strong-coupling regimes have been compared.

Three samples were investigated, each elaborated by spin coating an active layer onto a 45 nm silver film thermally evaporated on a glass cover slip. The active layer of the first sample (sample A) is composed by widely separated fluorescent polystyrene microspheres, emitting at 560 nm and having a diameter of 100 nm. The distance between each microsphere is sufficient to consider the emission of an insulated nanoparticle. The second sample (sample B) contains a continuous layer of CdSe quantum dots emitting around 660 nm. The distance between the quantum dots is smaller than the resolution of our setup, so that an uniform emission pattern will appear on the images. From the dispersion relations obtained by reflectometry measurements on these two samples, it has been checked that both kind of emitters are in the weak-coupling regime with the SP (data not shown) [21]. In the third sample (sample C), the optically active component is a *J*-aggregated 5, 5′, 6, 6′-tetrachloro-1, 1′-diethyl-3, 3′-di(4-sulfobutyl)-benzimidazolo-carbo cyanine (TDBC). The TDBC layer is formed by an ensemble of linear *J*-aggregate chains with a small length compared to the wavelength and, thus, can be seen as a set of independent emitters randomly spread throughout the film. Figure 1(b) presents the reflectometry experiment recorded in the Fourier space for sample C. The measured dispersion relation presents an anticrossing characteristic of a strong-coupling regime between the SP and the TDBC exciton, as previously reported for this kind of sample [8]. The Rabi splitting energy calculated with a classical two-level oscillator model is 300 meV.

In a first set of experiments, the emission through the silver layer for each sample was imaged on the CCD camera. For sample A in the k_{total} configuration [Fig. 2(a)], the emission of one microsphere forms two lobes oriented in the vertical direction. When the beam block is inserted in the Fourier plane (k_{up}), only the radiation having wave vector components in the upper half-plane is detected. In this case, the lower emission lobe is suppressed [Fig. 2(b)]. These images can be clearly interpreted in terms of a localized particle emitting SPs propagating upwards and downwards [Fig. 2(a)] or only upwards [Fig. 2(b)]. The same behavior is observed for sample B [Figs. 2(c) and 2(d)]. In these images, the bright central area corresponds to a collection of CdSe quantum dots excited by the

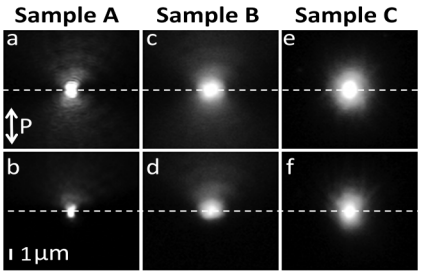

FIG. 2. Direct images of the surface leakage radiation for the different samples: (a),(b) sample A (insulated microspheres); (c), (d) sample B (CdSe nanocristals); (e),(f) sample C (TDBC layer in strong coupling). Panels (a), (c), and (e) correspond to the k_{total} detection, and panels (b), (d), and (f) to k_{up} detection configuration. The vertical arrow indicates the polarization direction *P*. The horizontal dotted lines correspond to the position of the emission center.

laser beam. The emission pattern presents two lobes, the lower one being suppressed in the k_{up} configuration [Fig. 2(d)]. The set of emitters in the weak-coupling regime with SP modes behaves as a sum of independently emitting particles. The recorded emission patterns are drastically different when the emitters are in the strong-coupling regime with SPs, exhibited by sample C [Figs. 2(e) and 2(f)]. In this case, the emission pattern has an oval shape in the k_{total} configuration and is only slightly modified in the k_{up} configuration. An important observation here is that the lower lobe persists in the k_{up} configuration. This suggests that the emission cannot be interpreted in terms of a set of particles which independently emit propagating SPs, as in sample B in weak coupling, but rather arises from an ensemble of many emitters all coupled to the same SP; together, they comprise an extended hybridized polaritonic state. The precise shape of the pattern should be related to details of the relaxation process from higher energy local Frenkel excitons into extended polaritonic states. One can envision different scenarios such as the initial formation of a local polariton wave packet, which would then rapidly extend, or a more direct relaxation into extended polaritons. Some theoretical studies of the dynamics of polariton wave packets in disordered systems in strong coupling have been performed [14] indicating a strong dependence on system parameters; these issues are, however, out of scope of this Letter.

In order to study the spatial coherence of this emitter assembly, two Young slits are inserted in an intermediate image plane of the sample. The Young slits are obtained by crossing a vertical slit with two V-shaped slits in order to vary the interslit distance. The resulting slits, located on both sides of the excitation spot (FWHM 0.7 μm), select the emission from two regions of the sample separated by a distance of 2.8 μm. The interference pattern recorded from sample A (a single localized emitter) is shown in Fig. 3(a). Interference fringes appear on the image. This case is analogous to a classical wave front division interference experiment: The emitter generates SPs propagating upwards and downwards before reaching the spatial regions selected by the upper and lower slits. The radiation propagating along these two paths interferes on the entrance slit of the spectrometer. In the k_{up} configuration, however, which disables the lower direction of propagation, only the upper slit remains illuminated and the interference fringes disappear [Fig. 3(b)]. In the case of sample B, no fringes are visible in both configurations. This is what is expected for a set of independent localized emitters. Each of them generates its own interference pattern associated with a phase difference which depends on its position between the slits. As the excitation spot extends over 0.7 μm, a blurring of the fringes occurs.

In contrast to samples A and B, sample C displays interference patterns in both the k_{total} [Fig. 3(e)] and k_{up} [Fig. 3(f)] configurations between 610 and 645 nm,

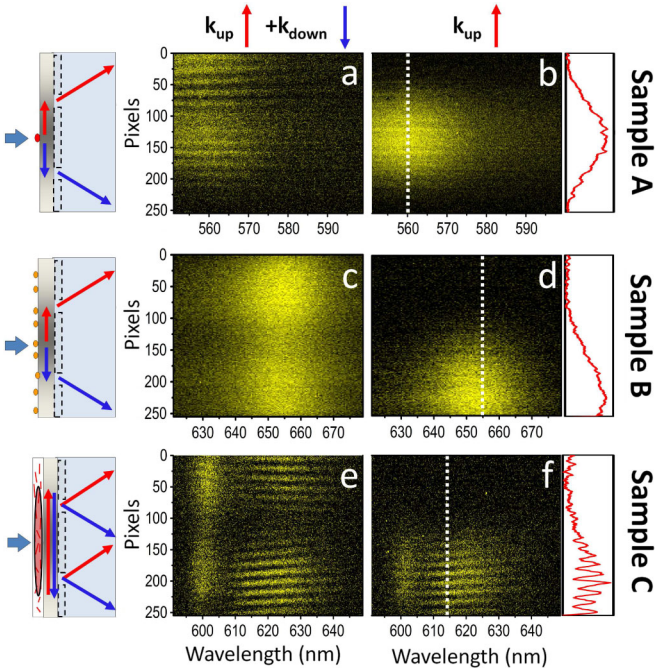

FIG. 3 (color online). Interference pattern recorded for samples A, B, and C: without selection on the wave vector [panels (a), (c), and (e), respectively] and with only the upwards propagation [panels (b), (d), and (f), respectively]. Layouts of different propagation mechanisms are drawn on the left side of the figure for each of the samples. For the (k_{up}) configuration, the intensity profile measured along the white dotted line is drawn on the right side of the figure.

corresponding to the SP-exciton mixed (polaritonic) states. The persistence of the interference fringes, even when the SP-assisted interferences are suppressed (k_{up}), demonstrates the spatial coherence of the extended hybrid states over a distance of 2.8 μm. The results may be compared to similar experiments performed on long polymer chains [16]. For those long molecules, the emission along the chain is coherent: The whole polymer chain emits even when excited with a localized spot. In a comparable manner, in our case a single dye chain cannot be excited independently from the others as shown in the diffusion experiments of Fig. 2.

The spatial extent of the SP-exciton hybrid states is now further addressed with a similar Young experiment but with a laser spot (FWHM 10 μm) covering both interfering regions on the sample. The emission pattern of a control sample consisting of a TDBC layer directly deposited on a glass cover slip without silver is shown in Fig. 4(a) and does not display any interference fringes, which agrees with the assertion that the TDBC layer is constituted by independent emitters formed by the aggregated dye chains. Interference images are recorded for sample C, a TDBC layer on silver [Fig. 4(b)]. Two different regions can be seen in the image: the polaritonic emission between 610 and 645 nm presenting interference fringes and the

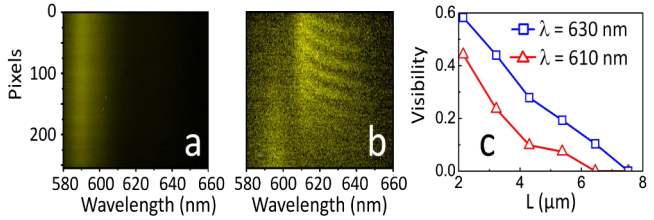

FIG. 4 (color online). (a) Emission pattern for a TDBC layer directly deposited on a glass substrate. (b) Typical interference pattern for a TDBC layer on silver with an excitation spot larger than the interslit distance (here 4.4 μm). (c) Visibility of the fringes as a function of the distance for two detection wavelengths (610 and 630 nm).

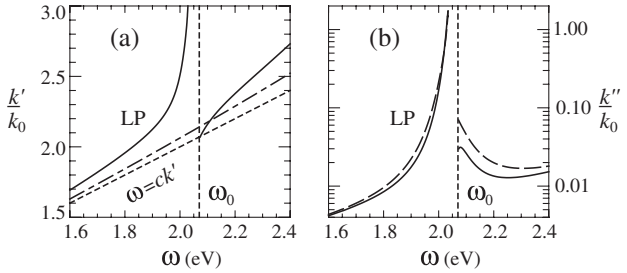

FIG. 5. Dispersion of surface polaritons in the vicinity of the resonance with the excitations of the thin layer: (a) real and (b) imaginary parts of the wave vector as a function of frequency in units of k_0, the wave number of the vacuum photon at 1 eV ($\lambda_0 \simeq 1240$ nm). The Rabi splitting of two polariton branches is clearly seen in panel (a), which also displays the bare (in the absence of the layer) SPs by a dash-dotted line. Numerical parameters used: $\omega_0 = 2.07$ eV, $\varepsilon_0 = 3.05$, $d = 20$ nm, $A = 2$ eV^2, $\delta_0 = 14$ meV, $\varepsilon_{2b} = 3.29$, $\omega_p = 8.93$ eV, and $\delta = 79$ meV. Dashed lines in panel (b) show the results for larger $\delta_0 = 25$ meV.

emission around 600 nm without interferences. The latter emission comes from incoherent states at the bare TDBC exciton energy. The existence of both incoherent and coherent extended states in the polariton spectrum has been discussed theoretically [13–15] for organic microcavities in the strong-coupling regime. Figure 4(c) presents the visibility of the fringes as a function of the distance between the interfering regions. For a detection wavelength of 630 nm the visibility vanishes at 7.5 μm, while for 610 nm the visibility decreases faster and vanishes around 6.5 μm, showing a reduction of the coherence length when the wavelength becomes closer to the bare exciton emission at 600 nm.

To elucidate the generic character and the origin of the frequency-dependent degree of coherence, we now provide an illustrative calculation of surface polaritonic states in a simpler parent system consisting of a thin (thickness d) resonating organic layer on a metallic substrate [22]. The dispersion equation, frequency ω vs in-plane wave vector k, can be found in this case as

$$\kappa_1/\varepsilon_1 + \kappa_2/\varepsilon_2 = \beta(k^2/\varepsilon_\perp - \omega^2/c^2 + \varepsilon_\parallel \kappa_1 \kappa_2/\varepsilon_1 \varepsilon_2),$$

where $\kappa_i^2 = k^2 - \varepsilon_i \omega^2/c^2$, $\beta = -\tanh(\kappa d)/\kappa$ and $\kappa^2 = (\varepsilon_\parallel/\varepsilon_\perp)k^2 - \varepsilon_\parallel \omega^2/c^2$. The dispersion equation features various ω-dependent dielectric functions, their imaginary parts being representative of the dissipation and disorder in the system. In the absence of the layer, $\beta = 0$, the dispersion equation would yield standard SP excitations at the interface between dielectric (we choose vacuum $\varepsilon_1 = 1$) and metallic [$\varepsilon_2 = \varepsilon_{2b} - \omega_p^2/\omega(\omega + i\delta)$] half-spaces. The organic layer here is anisotropic: For layered J aggregates we may assume that the resonance (frequency ω_0) occurs only for the polarization along the layer [$\varepsilon_\parallel = \varepsilon_0 + A/(\omega_0^2 - (\omega + i\delta_0)^2)$], while no resonance polarization takes place perpendicular to the layer ($\varepsilon_\perp = \varepsilon_0$).

Figure 5 shows the resulting two polaritonic branches in the form of the real and imaginary parts of the wave vector ($k = k' + ik''$) as functions of frequency ω in the vicinity of the resonance ω_0. Displayed are the states beyond the light line ($\omega < ck'$), which would be stationary states ($k'' = 0$) in the absence of the dissipation in the metal ($\delta = 0$) and the layer ($\delta_0 = 0$). It is the nonvanishing dissipation (disorder) that makes these states decaying, the decay length ($1/k''$) establishing the spatial scale of the coherence. We attribute the experimentally observed features to the behavior exhibited by the lower-energy polaritons (LP) in Fig. 5, where the decay length can indeed be in the micrometer range below the resonance frequency but strongly decreases upon the approach to the resonance. This trend agrees with the observations in Fig. 4, which clearly shows the disappearance of the coherence sufficiently close to the resonance. A more quantitative comparison with the measured values gives a good order of magnitude far from the resonance; 3 μm is found for both calculations and experiments at 630 nm but differs for energies very close to the resonance: At 610 nm the measured value is 1.6 μm, while the calculation expects 0.2 μm. This difference can be explained by the high steepness of the theoretical dispersion relation near the resonance [Fig. 5(b)]. A large variation of the coherence length can be induced by small energy variations inherent to the experiments: the spectrometer spectral resolution (2 nm for Fig. 4) and the position of the J-aggregated dye absorption which can shift a few nanometers depending on the elaboration conditions.

The formation of macroscopic coherent states is expected for a large number of disordered materials like organic dyes [8,11], layers of quantum dots [12], and rare earth ions [23] strongly coupled to SPs. The simple design of the samples enables the manipulation of these coherent states by structuring the active layer at distances shorter than the coherence length, by using patterns or inclusion of several different materials, opening a way to a new class of plasmonic materials.

The authors thank J. Bloch, R. Grousson, and M. Broyer for helpful discussions and support. This work has been

supported by the French ANR PNANO SCOP and by the Lyon Nanoptec center. V. M. A. acknowledges the hospitality of Scuola Normale Superiore (Pisa) via support of the European Commission (Grant No. FP7-PEOPLE-ITN-2008-237900 "ICARUS") and thanks Russian Foundation for Basic Research for partial support.

*joel.bellessa@univ-lyon1.fr

[1] A. V. Akimov *et al.*, Nature (London) **450**, 402 (2007).
[2] Y. Fedutik *et al.*, Phys. Rev. Lett. **99**, 136802 (2007).
[3] P. Anger, P. Bharadwaj, and L. Novotny, Phys. Rev. Lett. **96**, 113002 (2006).
[4] P. Andrew and W. L. Barnes, Science **306**, 1002 (2004).
[5] V. N. Pustovit and T. V. Shahbazyan, Phys. Rev. Lett. **102**, 077401 (2009).
[6] D. G. Lidzey *et al.*, Science **288**, 1620 (2000).
[7] D. G. Lidzey *et al.*, Phys. Rev. Lett. **82**, 3316 (1999).
[8] J. Bellessa *et al.*, Phys. Rev. Lett. **93**, 036404 (2004).
[9] J. Dintinger *et al.*, Phys. Rev. B **71**, 035424 (2005).
[10] Y. Sugawara *et al.*, Phys. Rev. Lett. **97**, 266808 (2006).
[11] T. K. Hakala *et al.*, Phys. Rev. Lett. **103**, 053602 (2009).
[12] D. E. Gomez *et al.*, Nano Lett. **10**, 274 (2010).
[13] V. M. Agranovich, M. Litinskaia, and D. G. Lidzey, Phys. Rev. B **67**, 085311 (2003).
[14] V. M. Agranovich and Y. N. Gartstein, Phys. Rev. B **75**, 075302 (2007).
[15] M. Litinskaya and P. Reineker, Phys. Rev. B **74**, 165320 (2006).
[16] F. Dubin *et al.*, Nature Phys. **2**, 32 (2005).
[17] B. Hecht *et al.*, Phys. Rev. Lett. **77**, 1889 (1996).
[18] A. Drezet *et al.*, Appl. Phys. Lett. **89**, 091117 (2006).
[19] R. Carminati and J. J. Greffet, Phys. Rev. Lett. **82**, 1660 (1999).
[20] R. Zia and M. L. Brongbergsma, Nature Nanotech. **2**, 426 (2007).
[21] It has to be noted that the CdSe quantum dots can switch from weak to strong coupling if their concentration is increased by 5 orders of magnitude [12]. Nevertheless, another material, namely, TDBC, has been chosen for experiments in strong coupling. Indeed, TDBC allows a Rabi splitting more than 4 times larger than the polariton linewidths, thus ensuring an interaction with plasmon largely prevailing the scattering and damping of the system.
[22] V. M. Agranovich and A. G. Malshukov, Opt. Commun. **11**, 169 (1974).
[23] M. Lipson and L. C. Kimerling, Appl. Phys. Lett. **77**, 1150 (2000).